Elasto-plastic large displacement analysis of framed structures

Hesham Ali Zien El Din
Structural Eng. Dept, Faculty of Engineering, Alexandria University, Alexandria, Egypt

In this paper elasto-plastic analysis of framed structures is formulated in the convected Eulerian system taking into account both the large displacement effects and the spread of material plasticity. Elasto-plastic cubic elements of fiber-type are formulated to account for the spread of material plasticity across the element section and along its length. The derived centroidal axial strain includes the effect of bowing and hence the formulation is capable of modeling the beam-column effect. Moreover the variation of the centroidal axial strain along the element length associated with the spread of material plasticity is taken into account. Three Gaussian integration sections are employed along the element length for the numerical integration of the internal virtual work to calculate the element local forces and the tangent stiffness matrix. A computer program is developed based on the present formulation considering both the geometric and material nonlinear effects. The developed computer program is verified through comparisons with experimental and theoretical results. The effect of the centroidal axial strain variation along the element length is assessed through several numerical comparisons. Finally, the ability of the present analysis to trace the behavior of framed structures under reversible loading is checked.

في هذا البحث يتم تكوين معادلات حل داخل نظام أويلر المحمول لتحليل المنشئات الاطارية آخذين في الاعتبار تأثيرا ت الأزاحات الكبيرة و انتشار تلدن المادة. يتم تكوين عناصر مرنة–لدنة من النوع النسيجى من الدرجة الثالثة لتأخذ فى الأعتبار أنتشار التلدن على كامل قطاع العنصر وعلى طولة. الانفعال المحورى المركزى المستنتج يشمل تأثير التقوس ولذلك يكون تكوين معادلات الحل قادر على تمثيل التأثير الكمرى–العمودى. علاوة على ذلك يتم أخذ تغير الانفعال المحورى المركزى على طول العنصر المصاحب لأنتشار تلدن المادة فى الاعتبار. يتم توظيف ثلاث قطاعات للتكامل بطريقة جاوس على طول العنصر وذلك لتكامل الشغل الداخلى الافتراضى عدديا وذلك لحساب قوى العنصر المحلية ومصفوفة الجساءة المماسة. تم تصميم برنامج حاسب آلى مبنى على معادلات الحل المذكورة آخذين فى الأعتبار تأثيرات المادة و التأثيرات الهندسية اللاخطية. تم التحقق من برنامج الحاسب الآلى المصمم من خلال المقارنة بنتائج معملية و نظرية. تم تقييم تأثير تغير الانفعال المحورى المركزى على طول العنصر من خلال مقارانات عددية عديدة. فى النهاية تم أختبار قدرة طريقة التحليل المذكورة فى هذا البحث على تتبع سلوك المنشئات الاطارية المعرضة لتحميل عكسى.

Keywords: Elasto-plastic analysis, Framed structures, Cubic formulation, Fiber-type, Reversible loading

1. Introduction

Two main approaches for elasto-plastic analysis of framed structures are found in the literature, namely the plastic hinge approach, [1-7], and the distributed plasticity approach [8-13]. In the first approach, plastic hinge approach, the analysis is greatly simplified where the material plasticity is assumed to be concentrated at selected points, typically at the ends of structural members. This transforms the original problem of a material plasticity to a problem of at most a finite number of plastic yield hinges. In many cases this type of analysis can be handeled effectively by considering the problem as one of a modified elastic structure, where the modification consists of a local change of stiffness at the active yield hinges. While the computation advantage of the plastic hinge approach is significant, such analysis is suitable for preliminary approximate study as it is unable to deal with the spread of material plasticity. Moreover the modeling of realistic stress-strain relationship in the context of plastic hinge approach is quite complex, which leads often to the simplifying assumption of elastic-perfectly plastic material [5,7].

In this paper, material plasticity is considered through the second approach, the distributed plasticity approach [13]. Fiber-type elasto-plastic cubic elements have been

used, where the spread of plasticity can be monitored across the element section through enough number of detailed fibers for the section. The spread of plasticity along the element length is monitored through three sections at the Gaussian integration points, [14,15]. The derived centroidal axial strain includes the effect of bowing which allows modeling the beam-column effect. Moreover, the variation of centroidal axial strain due to the spread of material plasticity along the element length is considered. The formulation is derived in the convected Eulerian system, [16], in which the local displacements are always referred to the deformed element chord. Element-based orientation vectors are used rather than nodal triad vectors, [17], which perimts the modeling of large local displacements. A computer program based on the present formulation has been developed and verified through several comparisons with experimental and theoretical results.

2. Elasto-plastic cubic formulation

The elasto-plastic cubic formulation is derived in the convected Eulerian system, where the element local displacements are referred to element chord in the deflected state to take into account the large displacement effect, as presented in ref. [16]. The material plasticity is considered through monitoring the stress-strain relation at enough number of fibers across the element sections at several locations along the element length defined by Gauss integration rule [15].

3. Local displacements & cubic interpolation functions

Six local degrees of freedom, referred to the element convected axes, are employed for three-dimensional formulation of framed structures, as shown in fig. 1. The local x-axis is the element chord in the deflected state connecting the centroids of the two end sections. The local y-axis and z-axis are the section principal axes. The element basic local displacements vector is ${}_c\mathbf{U}$;

$${}_c\mathbf{U} = [\theta_{1y}, \theta_{1z}, \theta_{2y}, \theta_{z2}, \Delta, \theta_T]^T \ . \quad (1)$$

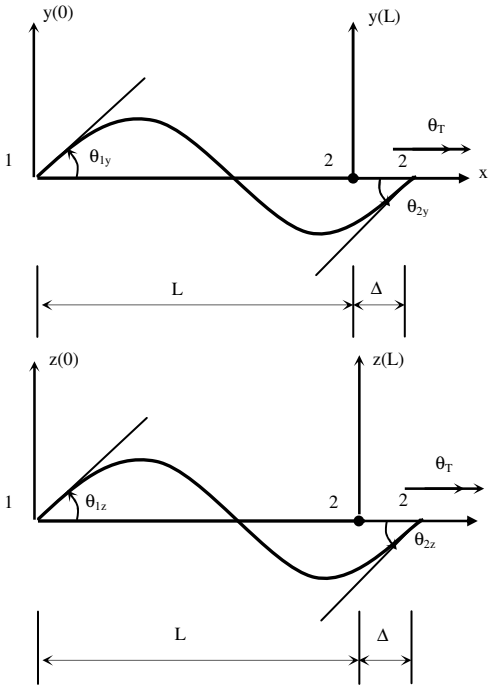

Fig. 1. Element local degrees of freedom referred to the element conveected axes.

The corresponding element basic local forces vector is ${}_c\mathbf{f}$;

$${}_c\mathbf{f} = [M_{1y}, M_{1z}, M_{2y}, M_{2z}, F, M_T]^T \ . \quad (2)$$

The centroidal axial displacement, $u(x)$, and the relative twist, $\alpha(x)$, at any point along the element reference axis, x-axis, are defined by linear interpolation functions as follows:

$$u(x) = \Delta.x / L, \quad (3)$$

$$\alpha(x) = \theta_T.x / L. \quad (4)$$

The centroidal displacement in the local y-direction, $v(x)$, and in the local z-direction, $w(x)$, at any point along the reference axis, x-axis, are defined by cubic interpolation functions, [13], given by;

$$v(x) = (\theta_{1y} + \theta_{2y}). (x^3/L^2) - (2\theta_{1y} + \theta_{2y}). (x^2/L) + \theta_{1y}.x \ , \quad (5)$$

$$w(x) = (\theta_{1z} + \theta_{2z}). (x^3/L^2) - (2\theta_{1z} + \theta_{2z}). (x^2/L) + \theta_{1z}.x. \quad (6)$$

4. Generalized strains

Through the derivation of the present formulation, the following assumptions are made:

a- Plane sections remain plane after deformation.

b- Warping strains due to non-uniform torsion are negligible.

c- Shear strains due to flexure are negligible.

d- The section centroid and shear center are coincident, and their loci represent the element reference axis.

These assumptions allow the strain state within a cross-section to be determined solely by a set of four generalized strains: centroidal axial strain, ε_c, rate of twist, ζ, and curvature strains about the two principal axes, κ_y and κ_z. The derivation of the centroidal axial strain includes the effect of bowing and hence the formulation is capable of modeling the beam-column effect. Moreover, the variation of ε_c along the element length due to spread of material plasticity is considered, rather than assuming it constant;

$$\varepsilon_c = du/dx + 0.5(dv/dx)^2 + 0.5(dw/dx)^2. \quad (7)$$

The remaining three generalized strains are obtained from the following differential relations:

$$\zeta = d\alpha/dx, \quad (8)$$

$$\kappa_y = d^2v/dx^2, \quad (9)$$

$$\kappa_z = d^2w/dx^2. \quad (10)$$

Substituting eqs. (3-6) into eqs. (7-10), the relationships between the generalized strains and the element freedoms are obtained as follows:

$$\begin{aligned}\varepsilon_c = (\Delta/L) &+ 4.5(\theta_{1y}^2 + \theta_{2y}^2 + 2\,\theta_{1y}\,.\,\theta_{2y} + \theta_{1z}^2 \\ &+ \theta_{2z}^2 + 2\,\theta_{1z}\,.\,\theta_{2z})(x/L)^4 - 6.0(2\theta_{1y}^2 \\ &+ \theta_{2y}^2 + 3\,\theta_{1y}\,.\,\theta_{2y} + 2\theta_{1z}^2 + \theta_{2z}^2 \\ &+ 3\,\theta_{1z}\,.\,\theta_{2z})(x/L)^3 + (11\theta_{1y}^2 + 2\theta_{2y}^2 \\ &+ 11\theta_{1y}\,.\,\theta_{2y} + 11\theta_{1z}^2 + 2\theta_{2z}^2 \\ &+ 11\theta_{1z}\,.\,\theta_{2z})(x/L)^2 - 2.0(2\theta_{1y}^2 \\ &+ \theta_{1y}\,.\,\theta_{2y} + 2\theta_{1z}^2 + \theta_{1z}\,.\,\theta_{2z})(x/L) \\ &+ (\theta_{1y}^2 + \theta_{1z}^2)/2.0, \end{aligned} \quad (11)$$

$$\zeta = \theta_T/L, \quad (12)$$

$$\kappa_y = 6.0\,(\theta_{1y}+\theta_{2y})\,.\,(x/L^2) - 2.0\,(2\theta_{1y} + \theta_{2y})/L, \quad (13)$$

$$\kappa_z = 6.0\,(\theta_{1z}+\theta_{2z})\,.\,(x/L^2) - 2.0\,(2\theta_{1z} + \theta_{2z})/L. \quad (14)$$

5. Generalized stresses

As the relationship between the generalized stresses and strains can not be established explicitly in the presence of material plasticity, the integration of the internal virtual work to get the element local forces is performed numerically. Three sections along the element length at the Gaussian integration points are employed for the numerical integration of the element internal virtual work. The positions of the three Gaussian sections according to Gauss integration rule [15] are:

$$\begin{aligned} {}_gx_1 &= 0.5L[1-(0.6)^{0.5}],\ {}_gx_2 = 0.5L, \\ {}_gx_3 &= 0.5L[1+(0.6)^{0.5}]\,. \end{aligned} \quad (15)$$

The corresponding weighting factors, a_g, at the three Gaussian sections required for the numerical integration process are:

$$a_1 = 5.0/9.0,\ a_2 = 8.0/9.0,\ a_3 = 5.0/9.0. \quad (16)$$

The generalized strains at the three Gaussian sections are represented by a matrix ${}_s\mathbf{U}$ as follows:

$${}_s\mathbf{U} = \begin{bmatrix} \varepsilon_c\,({}_gx_1) & \varepsilon_c({}_gx_2) & \varepsilon_c({}_gx_3) \\ \kappa_y\,({}_gx_1) & \kappa_y({}_gx_2) & \kappa_y({}_gx_3) \\ \kappa_z\,({}_gx_1) & \kappa_z\,({}_gx_2) & \kappa_z({}_gx_3) \\ \zeta & \zeta & \zeta \end{bmatrix}. \quad (17)$$

The elements of this matrix can be determined explicitly in terms of the element basic local displacements, ${}_c\mathbf{U}$, using eqs. (11-14).

Each Gaussian section is divided into a number of small areas at which strains and stresses are monitored, as shown in fig. 2. If the effect of shear strains on the material plasticity is neglected, only axial strains $e_{m,g}$ at the monitoring points of the Gaussian sections are considered as follows:

$$e_{m,g} = {}^4\textstyle\sum_{i=1}\, d_{m,i}\,.\,{}_sU_{i,g}, \quad (18)$$

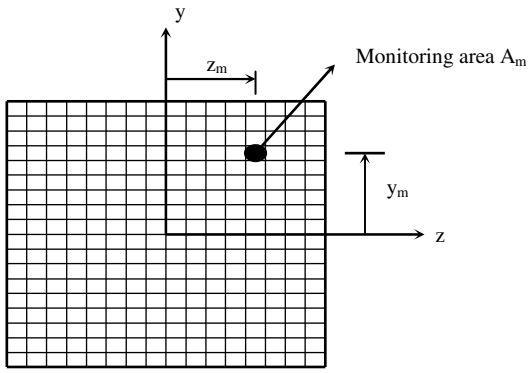

Fig. 2. Monitoring areas for a rectangular solid section.

where $e_{m,g}$ is the axial strain at a monitoring point m of Gaussian section g and,

$$d_{m,1} = 1,\ d_{m,2} = -y_m, d_{m,3} = -z_m \text{ and } d_{m,4} = 0. \quad (19)$$

A uniaxial stress-strain relationship is employed to establish the axial stress, $S_{m,g}$, at the monitoring points of the Gaussian sections in terms of axial strain $e_{m,g}$.

$$S_{m,g} = \sigma\,(e_{m,g}), \quad (20)$$

where σ is a function that represents the stress-strain relationship of the structure material.

For the element tangent stiffness matrix calculation needed for the incremental iterative solution procedure, the material tangent modulus ${}_tE_{m,g}$ at monitoring point m of Gaussian section g is:

$${}_tE_{m,g} = d\,S_{m,g} / d\,e_{m,g}. \quad (21)$$

Eventually the axial generalized stress ${}_sf_{1,g}$ and bending generalized stresses ${}_sf_{2,g}$ and ${}_sf_{3,g}$ at a Gaussian section g are determined from the material axial stress while the torsion generalized stress ${}_sf_{4,g}$ is determined from the torsion generalized strain as follows:

$$\begin{aligned} {}_sf_{i,g} &= {}^n\textstyle\sum_{m=1} A_m \,.\, d_{m,i} \,.\, S_{m,g}; \quad & i = 1, 2 \text{ and } 3 \\ {}_sf_{i,g} &= G \,.\, J \,.\, {}_sU_{i,g}; & i = 4, \end{aligned} \quad (22)$$

where A_m is the area of a monitoring point m, n is the number of monitoring points over a Gaussian section g, G is the elastic shear modulus and J is St Venant's torsion constant.

6. Element local forces and tangent stiffness

After the generalized stresses are determined at the three Gaussian sections along each element, the local end forces for each element can be obtained through numerical integration of internal virtual work and then carrying out the appropriate partial differentiation. Accordingly, the element local forces ${}_c\mathbf{f}$ corresponding to the element basic local displacements ${}_c\mathbf{U}$, defined by eqs. (1,2), are obtained as follows:

$${}_cf_i = {}^4\textstyle\sum_{J=1}\,{}^3\sum_{g=1} \quad a_g \,.\, {}_sf_{J,g} \,.\, {}_cT_{i,J,g}, \quad (23)$$

where ${}_c\mathbf{T}$ is a 6x4x3 matrix determined through partial differentiation of the generalized strains ${}_s\mathbf{U}$ with respect to local displacement ${}_c\mathbf{U}$, multiplied by (L/2).

$${}_cT_{i,J,g} = 0.5L(\,\partial_sU_{J,g} / \partial_cU_i). \quad (24)$$

Eventually the elements of ${}_c\mathbf{T}$ matrix can be determined explicitly in terms of the element basic local displacements as indicated in Appendix A.

The element local tangent stiffness matrix ${}_c\mathbf{K}$ can be obtained through partial differentiation of the element local forces ${}_c\mathbf{f}$ with respect to the element basic local displacements ${}_c\mathbf{U}$, where:

$${}_cK_{i,k} = \partial_cf_i / \partial_cU_k \,. \quad (25)$$

Substituting eq. (23) into eq. (25), we get:

$$\begin{aligned} {}_cK_{i,k} &= {}^4\textstyle\sum_{J=1}\,{}^3\sum_{g=1}\ (a_g \,.\, {}_cT_{i,J,g} \,.\, \partial_sf_{J,g} / \partial_cU_k \\ &+ a_g \,.\, {}_sf_{J,g} \,.\, \partial_cT_{i,J,g} / \partial_cU_k\,), \end{aligned} \quad (26)$$

$$\begin{aligned} {}_cK_{i,k} = {}^4\textstyle\sum_{J=1}{}^3\sum_{g=1}\, a_g.\, [{}_cT_{i,J,g} \,.\, {}^4\sum_{h=1}(\partial_sf_{J,g}/\,\partial_sU_{h,g}\,). \\ (\partial_sU_{h,g}/\,\partial_cU_k\,) + {}_sf_{J,g} \,.\, \partial_cT_{i,J,g}/\,\partial_cU_k], \end{aligned} \quad (27)$$

$$\begin{aligned} {}_cK_{i,k} = (L/2) \,.\, {}^4\textstyle\sum_{J=1}\,{}^3\sum_{g=1}\,{}^4\sum_{h=1}\, a_g.\, {}_cT_{i,J,g} \,. \\ {}_sK_{J,h,g} \,.\, {}_cT_{k,h,g} \quad + \quad {}_fK_{i,k}, \end{aligned} \quad (28)$$

where ${}_cT_{i,J,g}$ is defined in eq. (24) and

$$ {}_sK_{J,h,g} = (\partial_s f_{J,g} / \partial_s U_{h,g}), \quad (29) $$

$$ {}_fK_{i,k} = {}^4\sum_{J=1}{}^3\sum_{g=1} a_g . {}_sf_{J,g} . \partial_c T_{i,J,g} / \partial_c U_k . \quad (30) $$

Substituting eq. (22) into eq. (29), we get:

For Index: J =1,2,3 and h =1,2,3

$$ {}_sK_{J,h,g} = {}^n\sum_{m=1} A_m . d_{m,J} . (\partial S_{m,g} / \partial e_{m,g}) . (\partial e_{m,g} / \partial_s U_{h,g}) , \quad (31) $$

where A_m is the area of a small monitoring area on the element cross section and *index* n is the total number of monitoring areas that represents the real element cross section.

Using eq. (21) and eq. (18), we get:

$$ {}_sK_{J,h,g} = {}^n\sum_{m=1} A_m . d_{m,J} . {}_tE_{m,g} . (\partial\, {}^4\sum_{L=1} d_{m,L} . {}_sU_{L,g} / \partial_s U_{h,g}). \quad (32) $$

Thus for: J =1,2,3 and h =1,2,3 ;

$$ {}_sK_{J,h,g} = {}^n\sum_{m=1} A_m . d_{m,J} . {}_tE_{m,g} . d_{m,h} . \quad (33) $$

Substituting eq. (22) into eq. (29), we get:

For Index: J =4 and h =4

$$ {}_sK_{4,4,g} = G.J. \quad (34) $$

All other terms of ${}_s\mathbf{K}$ are zero.

Substituting the elements of ${}_c\mathbf{T}$ into eq. (30) and carrying out partial differentiation:

$$ {}_fK_{1,1} = {}_fK_{2,2} = {}_fK_{3,3} = {}_fK_{4,4} = 2F.L/15, $$
$$ {}_fK_{1,3} = {}_fK_{3,1} = {}_fK_{2,4} = {}_fK_{4,2} = -F.L/30, \quad (35) $$

where F is the axial force and all other terms of ${}_f\mathbf{K}$ are zero.

7. Developed computer program

A computer program based on the present formulation has been developed. The effect of large joint translations and rotations are considered through the convected Eulerian system. The Modified Newton-Raphson method together with the Current Stiffness Parameter are used to trace the nonlinear equilibrium path including the instability limit point, [16].

In the calculation of direct stresses at the monitoring points of each Gaussian section, strains at each iteration must be considered incrementally from the last equilibrium state, the end of last load increment. This requires storage of material variables (stresses, strains, etc) at the start of load increment, to be used as a reference to the new material variables calculated through each iteration. After global equilibrium is achieved at the end of load increment, the material variables are updated and saved.

8. Verification examples

The present formulation and the developed computer program are verified through comparisons with experimental and theoretical results of several examples.

Example 1

The experimental results of a K-frame shown in fig. 3 are reported in ref. [13]. The dimensions of the frame and the mechanical properties of the frame materials are indicated in the same figure. Both the transverse beam and diagonal members have circular tubular sections. An imperfection of (L/1000) are assumed in the diagonal members to initiate their possible lateral deflections. The nonlinear load-deflection relation, including the ultimate load and post-buckling behavior, is determined by the developed computer program, based on the present analysis, and compared with the published experimental result as shown in fig. 4. The difference between the predicted ultimate load and experimental one is less than 1%. Also, good result is obtained for the predicted post-buckling behavior as shown in fig. 4.

Example 2

Another validation example is a steel gable frame with solid circular section shown in fig.5. Experimental results of this frame have been reported in ref. [7], for symmetric loading case, e=0. The nonlinear load-deflection relationship is calculated by the present analysis and compared with the experimental

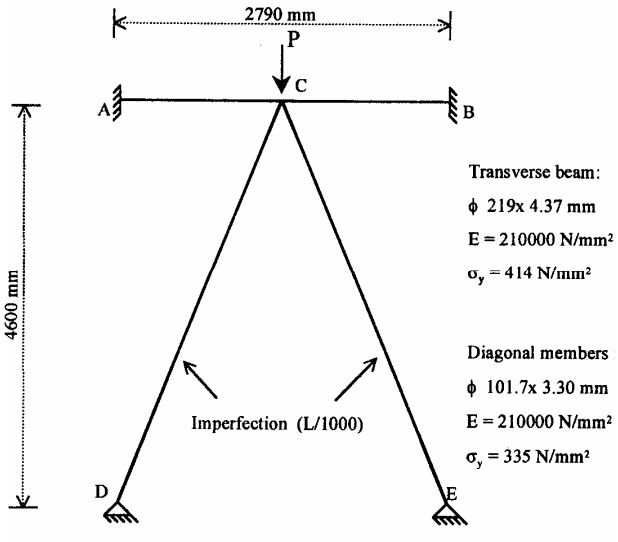

Fig. 3. Geometric configuration of K-frame.

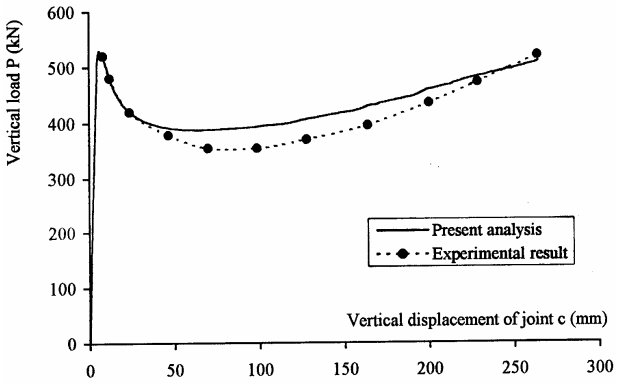

Fig. 4. Load-deflection relation of K-frame.

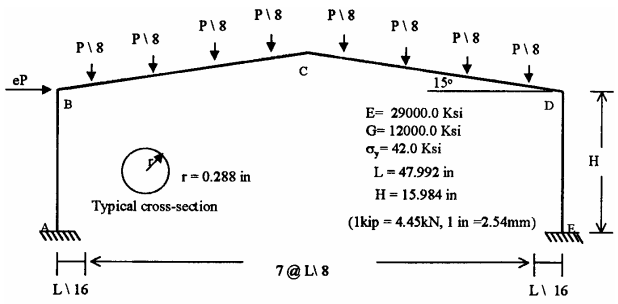

Fig. 5. Gable frame: dimensions and properties.

result, shown in fig. 6. A very small imperfection, e =0.001, is assumed with the numerical solution. Fair agreement with the experimental results is obtained although the maximum difference reaches 8%. This may be attributed to modeling the supports as totally

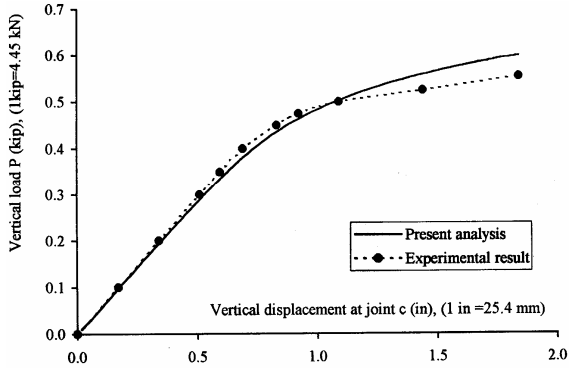

Fig. 6. Load-deflection relation of Gable frame.

fixed in the theoretical solution, while it is difficult to achieve complete fixation in practice especially with large deformation and spread of material plasticity.

Example 3

This example is a space curved frame consists of two semicircles in two perpendicular planes as shown in fig. 7. The curved space frame has a steel tubular circular section. Both the geometrical details and the mechanical properties of the used steel are indicated in fig. 7. The load-deflection curve is determined by the present analysis and compared with the solution of the commercial program Abaqus, [18], which considers both the geometric and material nonlinearity. Good agreement is obtained between the result of the present analysis and the solution of Abaqus as shown in fig. 8. The difference in predicting the ultimate load, between the two solutions is 1.7%. Also, good agreement in predicting the post-buckling behavior by the present analysis and Abaqus solution is achieved with maximum difference 4%.

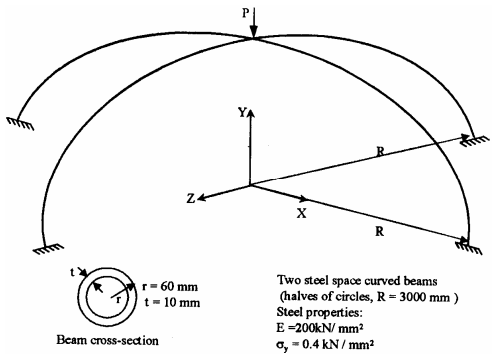

Fig. 7. Space curved frame of two semicircles.

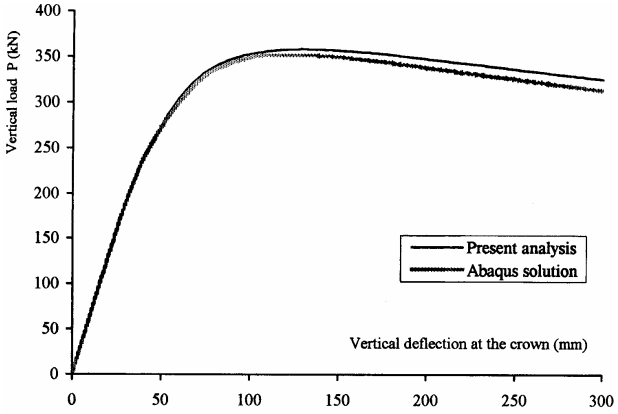

Fig. 8. Load-deflection relation of space curved frame.

Example 4

A space horizontal bent which consists of two steel straight members with tubular circular section, shown in fig. 9, is analyzed using Abaqus and the present formulation. The result is shown in fig. 10, where good agreement between the two solutions is obtained with maximum difference 2.7%.

9. Effect of the variation of the centroidal axial strain

Considering the bowing effect on centroidal axial strain, eq. (7), results in a variable function of fourth degree indicated in eq. (11). Moreover in the presence of material plasticity, the centroidal axial strain is not constant along the element length, where it depends on the nonlinear distribution of axial stress over the element section.

In the present analysis, the variation of centroidal axial strain along the element length has been considered, though it may be insignificant. To assess the effect of the centroidal axial strain variation, it is assumed constant along the element length with average value as follows:

$$\varepsilon_c = \Delta/L + (1/L).\ {}_0\int^L (0.5(dv/dx)^2 + 0.5(dw/dx)^2).dx. \quad (36)$$

Substituting eqs. (5) and (6) in eq. (36), constant centroidal axial strain along the element length is obtained as:

$$\varepsilon_c = \Delta/L + \{2\,(\theta_{1y}^{\,2} + \theta_{2y}^{\,2} + \theta_{1z}^{\,2} + \theta_{2z}^{\,2}) - (\theta_{1y}.\,\theta_{2y} + \theta_{1z}.\,\theta_{2z})\}/\,30. \quad (37)$$

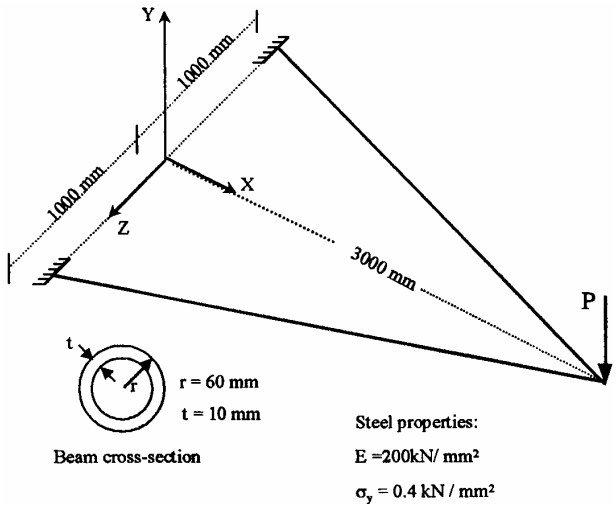

Fig. 9. Space horizontal bent of straight beams.

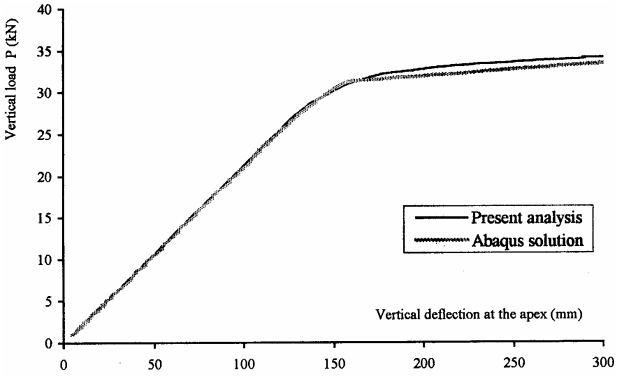

Fig. 10. Load-deflection relation of space horizontal bent.

Accordingly, some elements of the matrix ${}_c\mathbf{T}$ change as indicated in Appendix A.

The four previous verification examples are solved with the present analysis assuming *constant* centroidal axial strain and the results are compared with the solution considering *variable* centroidal axial strain, as shown in figs. 11, 12, 13 and 14. From the results, it can be seen that the effect of the variation of centroidal axial strain is very small, with maximum difference 3.2% obtained in example 4. This means that the variation of centroidal axial strain along the element length can be neglected and it can be assumed constant without any significant decrease in the solution accuracy.

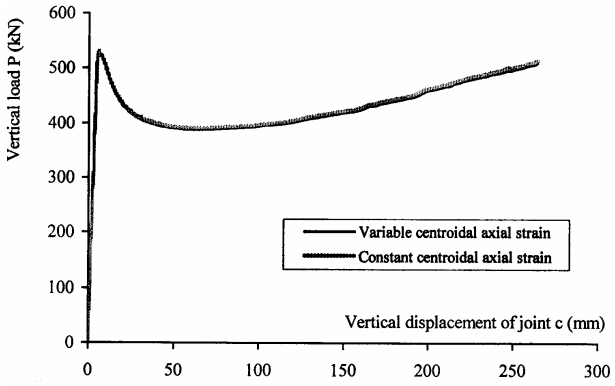

Fig. 11. Computed load-deflection relation of K-frame.

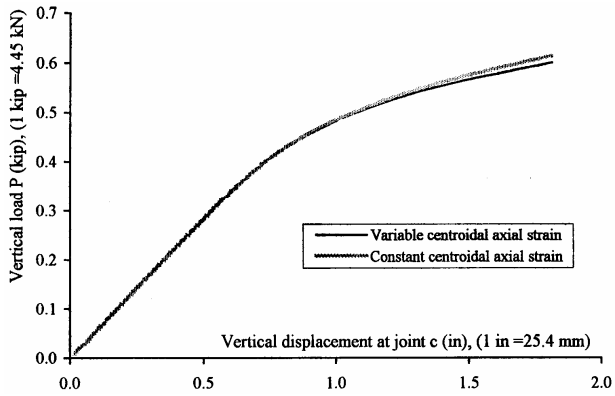

Fig. 12. Computed load-deflection relation of Gable frame.

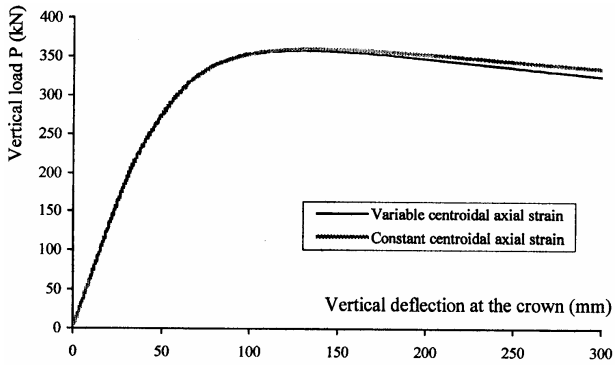

Fig. 13. Computed load-deflection relation of space curved frame.

10. Analysis with reversible loading

Elasto-plastic behavior of framed structures under reversible loading can be traced through the present analysis by applying the suitable cyclic stress-strain relationship of the used material at the monitoring points over each Gaussian section along the element length.

At the reversal points of a load-deflection curve, the load parameter and displacement increments are reversed with certain proportional elastic values and the overall stiffness of structure is updated according to the imposed displacement increments. Then the Modified Newton-Raphson iterative technique is applied till achieving the correct displacement increments through satisfying the equilibrium between the imposed external load and internal forces.

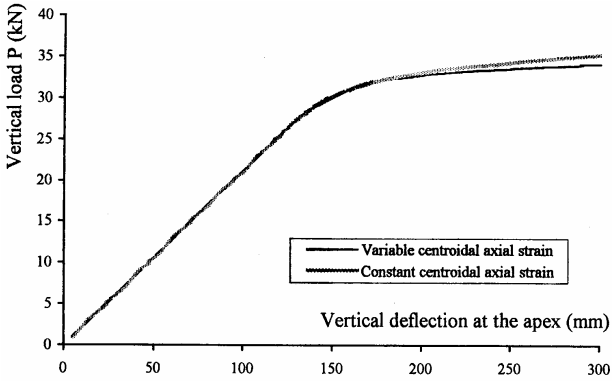

Fig. 14. Computed load-deflection relation of space horizontal bent.

Both the space curved frame, example 3, and the space horizontal bent, example 4, are analyzed by the present analysis using a kinematic model considering the material hardening and Bauschinger effect as shown in fig. 15. The results of the present analysis are compared with the solution of Abaqus, as indicated in fig. 16 and fig. 17. Good agreement between the result of the present analysis and Abaqus solution is achieved, though the difference at some parts of the shown load-deflection curves which is due to the Bauschinger effect considered in the present analysis through the used kinematic material model.

11. Conclusions

1. Elasto-plastic analysis for framed structures is formulated in the convected Eulerian system considering large displacement effects and spread of material plasticity. The elasto-plastic analysis is based on formulation of cubic elements of fiber-type which is capable

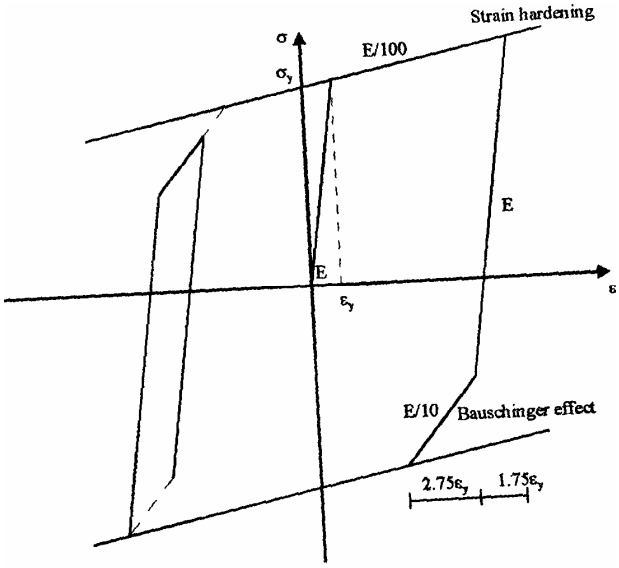

Fig. 15. Stress-strain model of steel under cyclic loading.

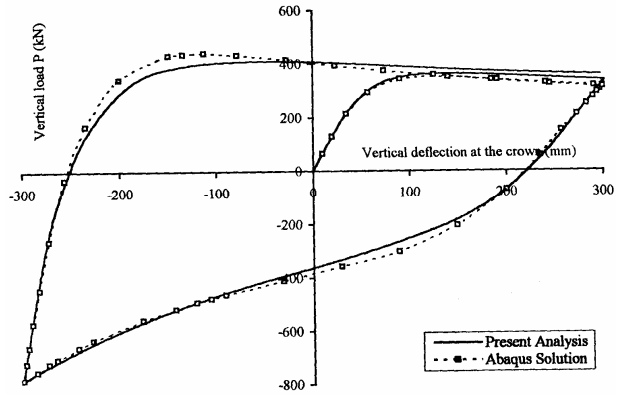

Fig. 16. Space curved frame under reversible loading.

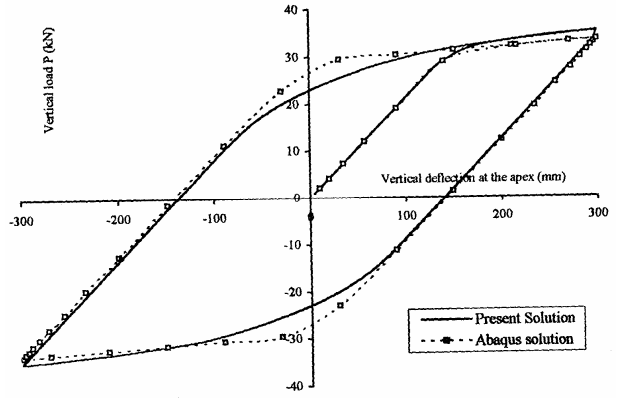

Fig. 17. Space horizotal bent under reversible loading.

to monitor the spread of material plasticity over the element section and along its length.

2.A computer program based on the present formulation is developed and verified through several comparisons with experimental and theoretical results.

3.The effect of the variation of the centroidal axial strain along the element length, due to considering bowing and spread of material plasticity, is assessed and according to the present results it is concluded that the centroidal axial strain variation can be neglected and assumed constant along the element length without any significant decrease in the solution accuracy.

4.The present elasto-plastic analysis is capable to trace the load-deflection path of framed structures under reversible loading through applying the suitable cyclic stress-strain relationship of the used material at the monitoring points over each Gaussian section along the element length.

Appendix A

The elements of ${}_c\mathbf{T}$ matrix, considering variable centroidal axial strain:

${}_cT_{1,1,1} = L.(0.1724\ \theta_{1y} - 0.055\ \theta_{2y})$

${}_cT_{1,1,2} = L.(0.03125\ \theta_{1y} + 0.03125\ \theta_{2y})$

${}_cT_{1,1,3} = L.(0.0176\ \theta_{1y} - 0.055\ \theta_{2y})$

${}_cT_{1,2,1} = -1.6619$, ${}_cT_{1,2,2} = -0.5$, ${}_cT_{1,2,3} = 0.6619$

${}_cT_{2,1,1} = L.(0.1724\ \theta_{1z} - 0.055\ \theta_{2z})$

${}_cT_{2,1,2} = L.(0.03125\ \theta_{1z} + 0.03125\ \theta_{2z})$

${}_cT_{2,1,3} = L.(0.0176\ \theta_{1z} - 0.055\ \theta_{2z})$

${}_cT_{2,3,1} = -1.6619$, ${}_cT_{2,3,2} = -0.5$, ${}_cT_{2,3,3} = 0.6619$

${}_cT_{3,1,1} = L.(0.0176\ \theta_{2y} - 0.055\ \theta_{1y})$

${}_cT_{3,1,2} = L.(0.03125\ \theta_{2y} + 0.03125\ \theta_{1y})$

${}_cT_{3,1,3} = L.(0.1724\ \theta_{2y} - 0.055\ \theta_{1y})$

${}_cT_{3,2,1} = -0.6619$, ${}_cT_{3,2,2} = 0.5$, ${}_cT_{3,2,3} = 1.6619$

${}_cT_{4,1,1} = L.(0.0176\ \theta_{2z} - 0.055\ \theta_{1z})$

${}_cT_{4,1,2} = L.(0.03125\ \theta_{2z} + 0.03125\ \theta_{1z})$

${}_cT_{4,1,3} = L.(0.1724\ \theta_{2z} - 0.055\ \theta_{1z})$

${}_cT_{4,3,1} = -0.6619$, ${}_cT_{4,3,2} = 0.5$, ${}_cT_{4,3,3} = 1.6619$

${}_cT_{5,1,1} = {}_cT_{5,1,2} = {}_cT_{5,1,3} = 0.5$

${}_cT_{6,4,1} = {}_cT_{6,4,2} = {}_cT_{6,4,3} = 0.5$

All other elements of ${}_c\mathbf{T}$ matrix are zero.

The elements of ${}_c\mathbf{T}$ matrix, considering constant centroidal axial strain:

${}_cT_{1,1,1} = {}_cT_{1,1,2} = {}_cT_{1,1,3} = L.(4\theta_{1y} - \theta_{2y})/60$

${}_cT_{2,1,1} = {}_cT_{2,1,2} = {}_cT_{2,1,3} = L.(4\theta_{1z} - \theta_{2z})/60$

${}_cT_{3,1,1} = {}_cT_{3,1,2} = {}_cT_{3,1,3} = L.(4\theta_{2y} - \theta_{1y})/60$

${}_cT_{4,1,1} = {}_cT_{4,1,2} = {}_cT_{4,1,3} = L.(4\theta_{2z} - \theta_{1z})/60$

All other elements of ${}_c\mathbf{T}$ matrix remain unchanged, with the same values as the case of variable centroidal axial strain.

References

[1] R.K. Wen, and F. Farhoomand "Dynamic Analysis of Inelastic Space Frames." J. Engng. Mech. Div., ASCE, 96, (EM5), pp. 667-686 (1970).

[2] S.A. Anagnostopoulos, "Inelastic Beams for Seismic Analysis of Structure." J.Struct. Div., ASCE, Vol. 107, (ST7), pp.1297-1311 (1981).

[3] Y. Ueda, and T. Yao, "The Plastic Node Method: A New Method of Plastic Analysis." J. Computer Methods Appl. Mech. Engng, Vol. 34, pp. 1089-1104 (1982).

[4] G.H. Powell, and P.F. Chen "3D Beam-Column Element with Generalized Plastic Hinges." J. Engng Mech., ASCE, Vol. 112 (7), pp. 627-641 (1986).

[5] B.A. Izzuddin, and A.S. Elnashai, "Adaptive Space Frame Analysis. Part I: A Plastic Hinge Approach." Proc. Instn. Civ. Engrs Structs & Bldgs, Vol. 99, pp. 303-316 (1993).

[6] S. Krenk, S. Vissing, and C. Jorgensen, "A Finite Step Updated Method for Elasto-Plastic Analysis of Frames.", J. Engng. Mech., ASCE, Vol. 119 (12), pp. 2478-2495 (1993).

[7] R. Abbasnia, and A. Kassimali, "Large Deformation Elastic-Plastic Analysis of Space Frames" J. Construct. Steel Research, Vol. 35, pp.275-290 (1995).

[8] R.E. Hobbs, and A.M. Jowharzadeh, "An Incremental Analysis of Beam-Columns and Frames Including Finite Deformations and Bilinear Elasticity" J. Comp. Struct., Vol. 9, pp. 323-330 (1978).

[9] T.Y. Yang, and S. Saigal, "A Simple Element for Static and Dynamic Response of Beams with Material and Geometric nonlinearities" Int. J. Num. Meth. Engng., Vol. 20, pp. 851-867 (1984).

[10] L. Corradi, and W.F. Chen, "A Refined Finite Element Model for the Analysis of Elastic-Plastic Frames" Int. J. Num. Meth. Engng., Vol. 20, pp. 2155-2174 (1984).

[11] H. Sugimoto, and W.F. Chen, " Inelastic Post-Buckling Behavior of Tubular Members" J. Struct. Engng., ACSE, Vol. 111 (9), pp. 1965-1978 (1985).

[12] J.L. Meek, and S. Loganathan, "Geometric and Material Nonlinear Behavior of Beam-Columns', J. Comp. Struct., Vol. 34, (1), pp. 87-100 (1990).

[13] B.A. Izzuddin, and A.S. Elnashai, "Adaptive Space Frame Analysis. Part II: A Distributed Plasticity Approach." Proc. Instn Civ. Engrs Structs & Bldgs, Vol. 99, Aug., pp.317-326 (1993).

[14] E. Hinton, and D.R. Owen, Finite Element Programming Academic Press Inc. (london) LTD (1977).

[15] B. Irons, and N.G. Shrive, Numerical Methods in Engineering and Applied Science, Ellis Horwood Limited, Chichester (1987).

[16] H.A. Zien El Din, "Analysis of Space Frames with Large Joint Rotations" The Eighth Arab Structural Engineering Conference, Cairo, 21-23 October, pp. 67-84 (2000).

[17] B. A. Izzuddin, et al., "Eulerian Formulation For Large-Displacement Analysis of Space Frames ." J. Engng. Mech., ASCE, Vol. 119 (3), pp.549-569 (1993).

[18] Hibbitt, Karlsson and Sorensen, Inc. Abaqus-Standard Users Manual, Detroit, USA (2001).

Received January 23, 2003
Accepted March 31, 2003